Figure S1

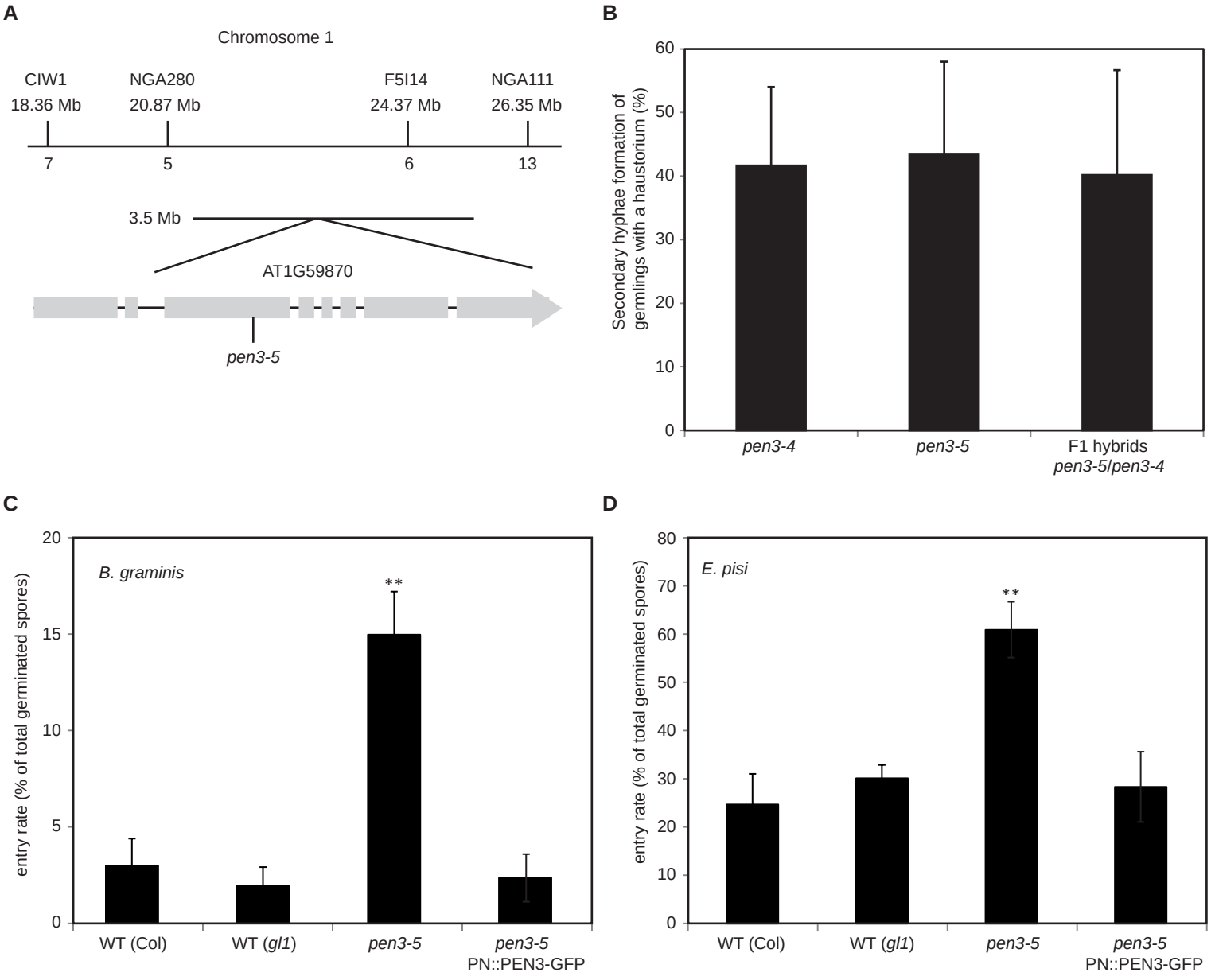
A
Chromosome 1
CIW1
18.36 Mb
NGA280
20.87 Mb
F5I14
24.37 Mb
NGA111
26.35 Mb
7
5
6
13
3.5 Mb
AT1G59870
pen3-5
B
Secondary hyphae formation of germlings with a haustorium (%)
60
50
40
30
20
10
0
pen3-4
pen3-5
F1 hybrids
pen3-5/pen3-4
C
B. graminis
entry rate (% of total germinated spores)
20
15
10
5
0
**
WT (Col)
WT (gl1)
pen3-5
pen3-5
PN::PEN3-GFP
D
E. pisi
entry rate (% of total germinated spores)
80
70
60
50
40
30
20
10
0
**
WT (Col)
WT (gl1)
pen3-5
pen3-5
PN::PEN3-GFP

Figure S2

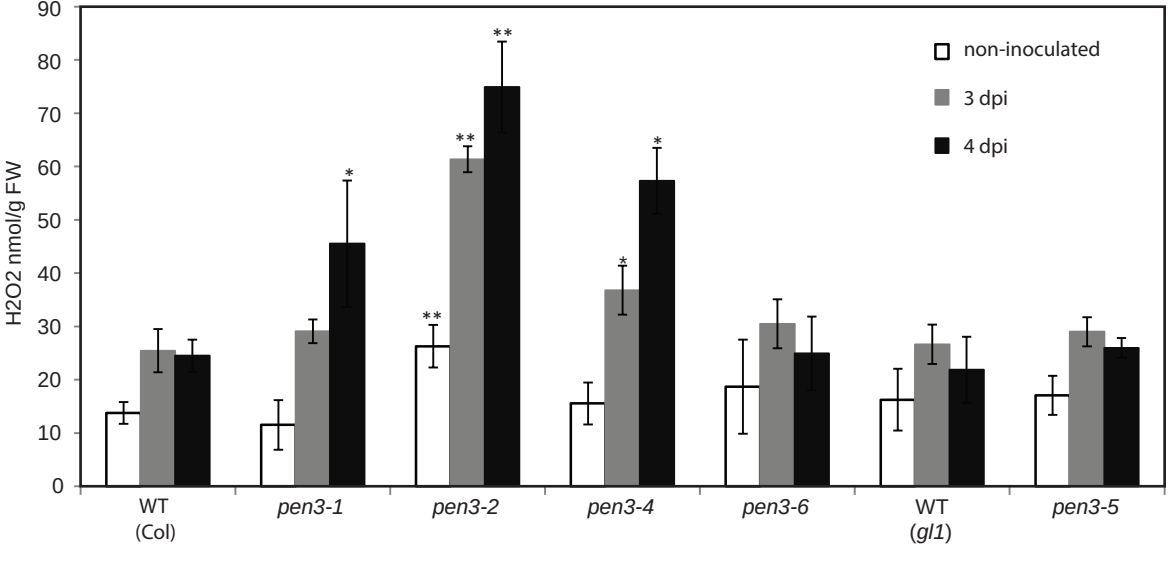
H2O2 nmol/g FW
90
80
70
60
50
40
30
20
10
0
non-inoculated
3 dpi
4 dpi
**
**
**
*
*
*
WT (Col)
pen3-1
pen3-2
pen3-4
pen3-6
WT (gl1)
pen3-5

Figure S3

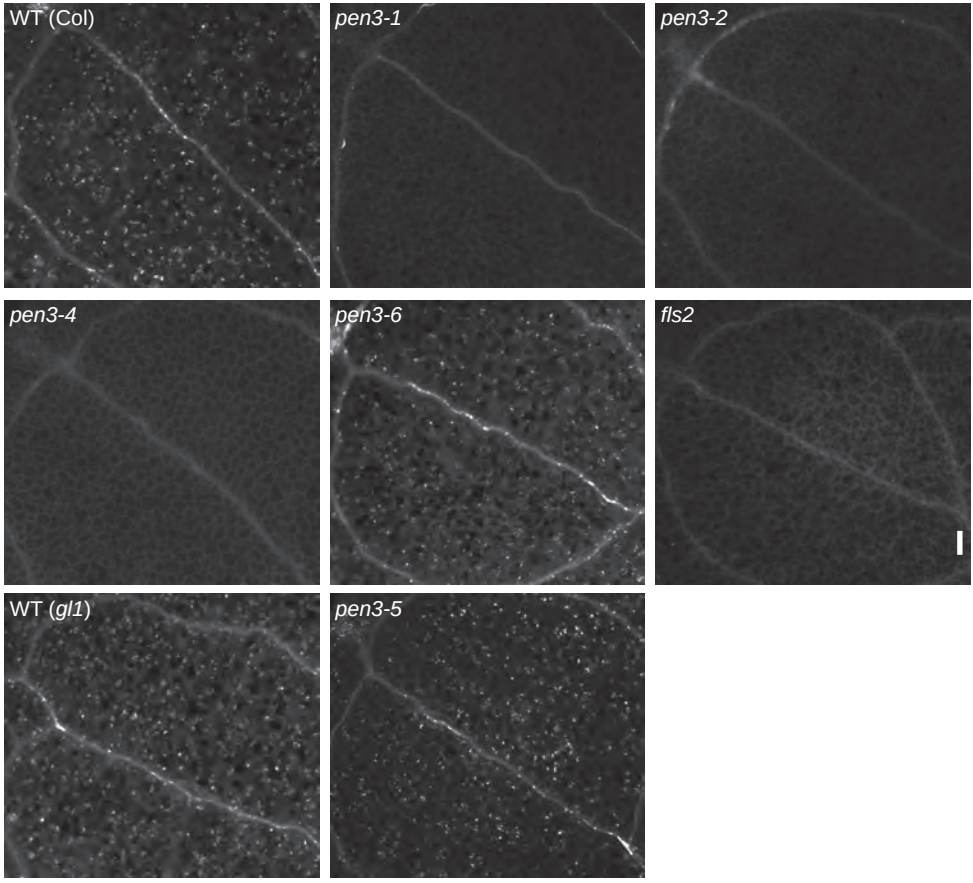

Figure S4

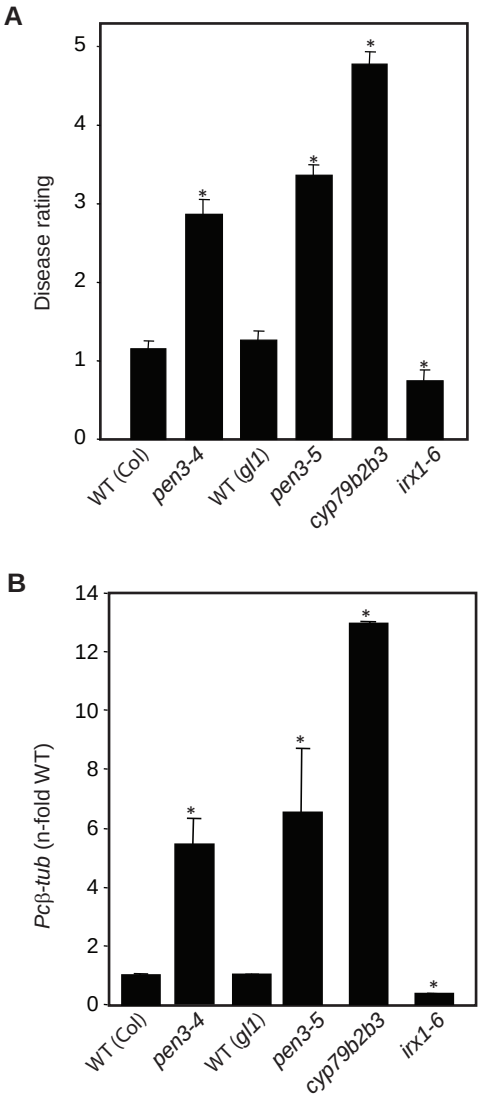
A
Disease rating
0
1
2
3
4
5
*
*
*
*
WT (Col)
pen3-4
WT (gl1)
pen3-5
cyp79b2b3
irx1-6
B
Pcβ-tub (n-fold WT)
0
2
4
6
8
10
12
14
*
*
*
*
WT (Col)
pen3-4
WT (gl1)
pen3-5
cyp79b2b3
irx1-6

Figure S5

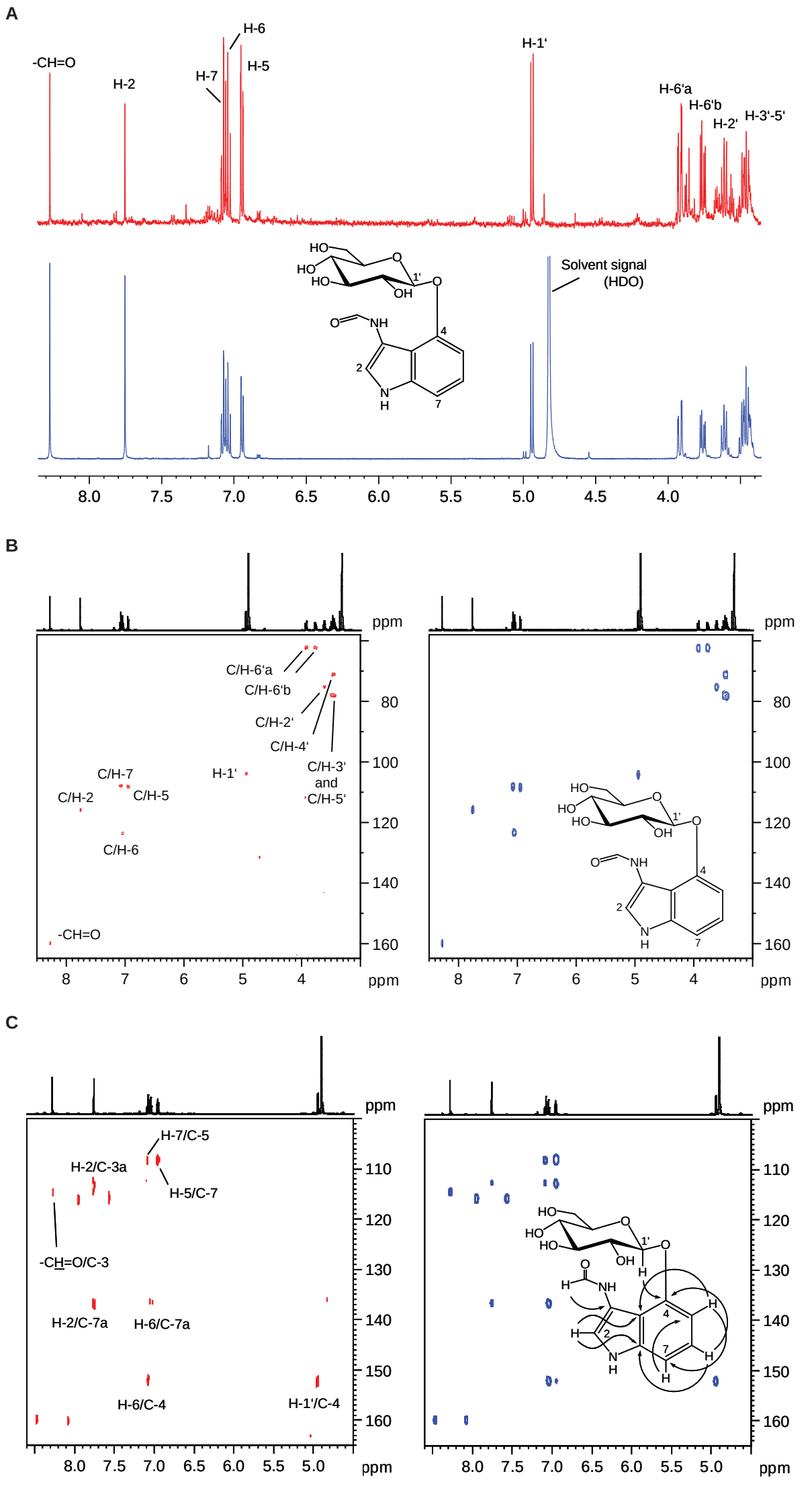
A
-CH=O
H-2
H-7
H-6
H-5
H-1‘
H-6‘a
H-6‘b
H-2‘
H-3‘-5‘
Solvent signal
(HDO)
8.0
7.5
7.0
6.5
6.0
5.5
5.0
4.5
4.0
B
ppm
C/H-6‘a
C/H-6‘b
C/H-2‘
C/H-4‘
C/H-3‘
and
C/H-5‘
H-1‘
C/H-7
C/H-2
C/H-5
C/H-6
-CH=O
80
100
120
140
160
8
7
6
5
4
C
H-7/C-5
H-2/C-3a
H-5/C-7
-CH=O/C-3
H-2/C-7a
H-6/C-7a
H-6/C-4
H-1‘/C-4
110
120
130
140
150
160
8.0
7.5
7.0
6.5
6.0
5.5
5.0

Figure S6

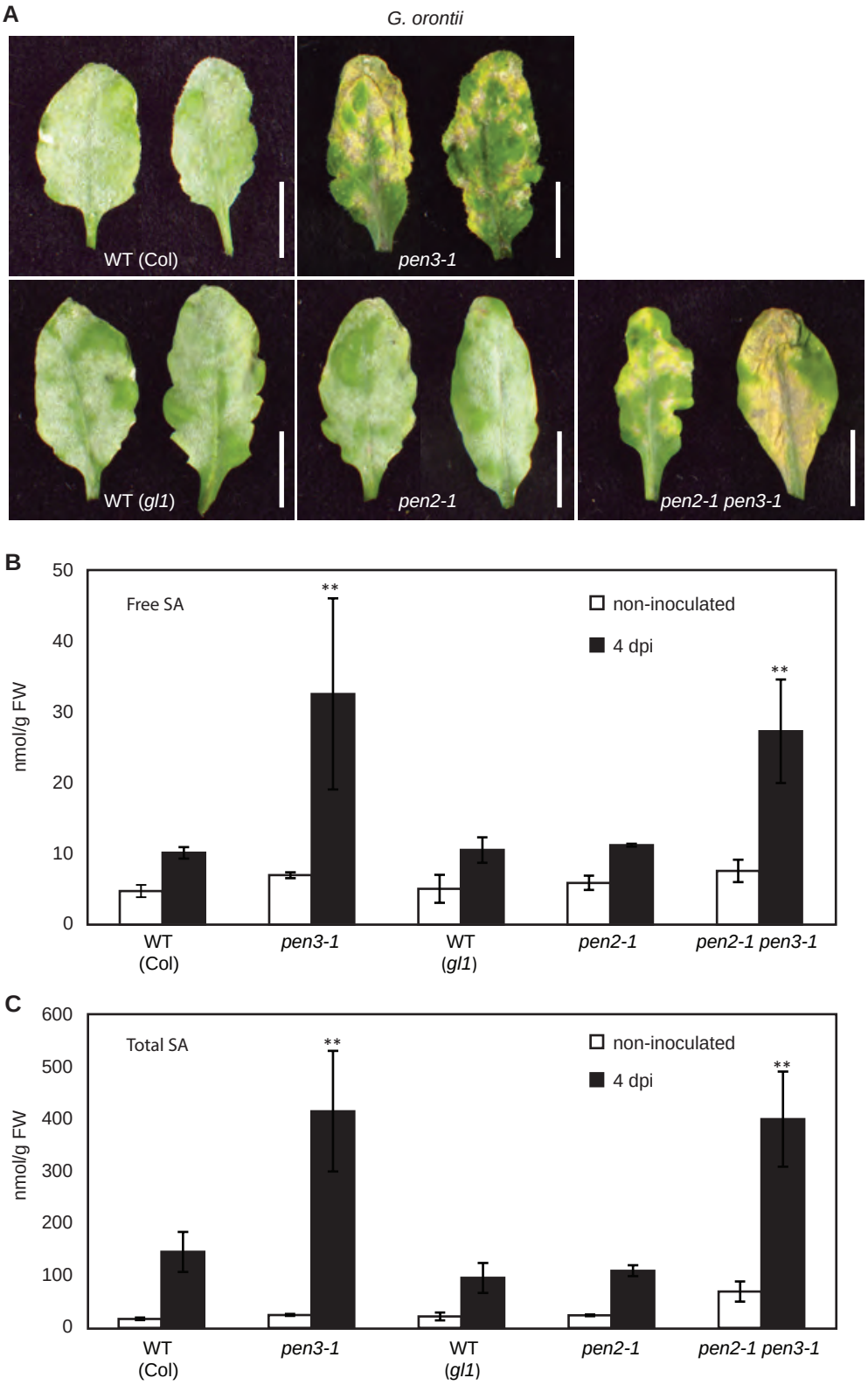
A
G. orontii
WT (Col)
pen3-1
WT (gl1)
pen2-1
pen2-1 pen3-1
B
Free SA
non-inoculated
4 dpi
nmol/g FW
50
40
30
20
10
0
**
**
WT (Col)
pen3-1
WT (gl1)
pen2-1
pen2-1 pen3-1
C
Total SA
non-inoculated
4 dpi
nmol/g FW
600
500
400
300
200
100
0
**
**
WT (Col)
pen3-1
WT (gl1)
pen2-1
pen2-1 pen3-1

Figure S7

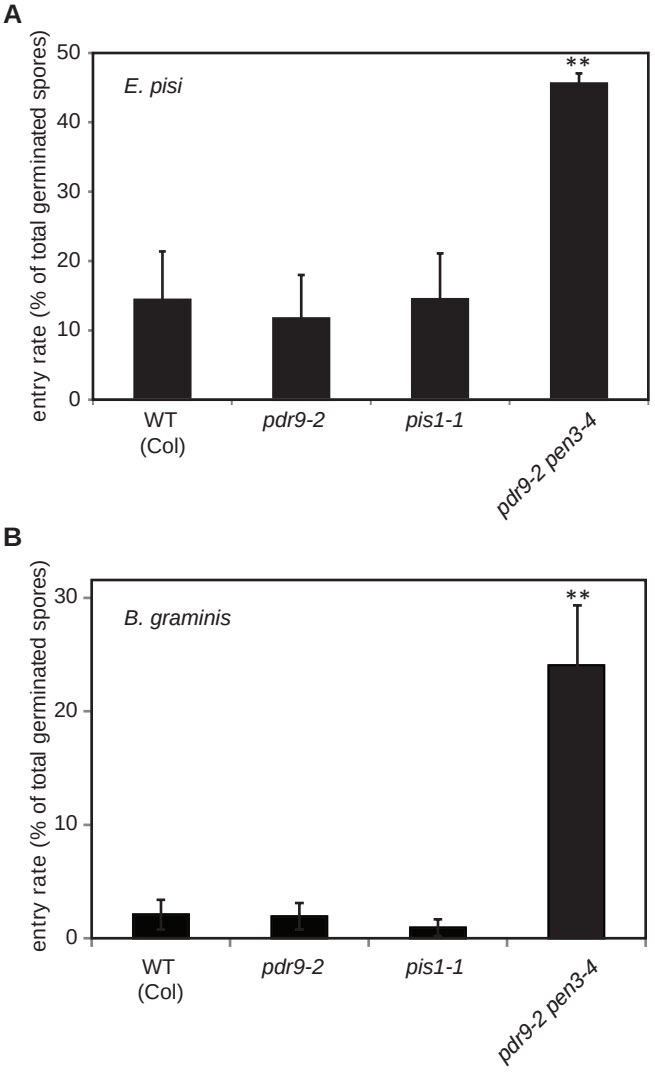
A
E. pisi
entry rate (% of total germinated spores)
50
40
30
20
10
0
**
WT (Col)
pdr9-2
pis1-1
pdr9-2 pen3-4
B
B. graminis
entry rate (% of total germinated spores)
30
20
10
0
**
WT (Col)
pdr9-2
pis1-1
pdr9-2 pen3-4

Supplementary experimental procedures

Plant material and growth conditions

We generated complementation lines by crossing *pen3-5* plants with a transgenic line expressing functional PEN3-GFP with native 5' regulatory PEN3 sequences in the *pen3-1* background (Stein et al., 2006). F_1 hybrids were validated for the presence of both *pen3-1* and *pen3-5* alleles using allele-specific PCR primers. Multiple F_2 plants were isolated after selection on kanamycin medium. The F_2 plants were subsequently genotyped for individuals lacking the *pen3-1* allele using allele-specific PCR primers. These plants were considered as *pen3-5* homozygotes carrying the PEN3-GFP transgene.

MS and NMR analysis

For LC-MS analysis the Ultimate 3000 series RSLC (Dionex, Sunnyvale, CA, USA) system and the Orbitrap XL mass spectrometer (Thermo Fisher Scientific, Bremen, Germany) operating at 35 000 and 7 500 HWPM resolution in MS and MS/MS mode, respectively, were used. Other conditions were similar as previously published (Bednarek et al., 2011).

^{1}H nuclear magnetic resonance (^{1}H NMR), ^{1}H-^{1}H correlated spectroscopy (^{1}H-^{1}H COSY), heteronuclear single quantum coherence (HSQC) and heteronuclear multiple bond correlation (HMBC) spectra were recorded on an Avance 500 NMR spectrometer (Bruker, Karlsruhe, Germany) at 300 K using a 5 mm TCI CryoProbe^{TM}. A double presaturation 1D NOESY pulse sequence (lc1pnf2; mixing time 100 ms) was used to suppress residual signals of water and methanol in the spectrum of the isolated sample. Chemical shift values (δ) are given relative to tetramethylsilane (TMS) as an internal standard, coupling constants in Hertz (Hz).

NMR data

^{1}H NMR (500 MHz, MeOH-d_4): δ 8.28 (1H, s, CHO), 7.76 (1H, s, H-2), 7.09 (1H, dd, *J* = 8.1, 1.1 Hz, H-7), 7.05 (1H, dd, *J* = 8.1, 7.5 Hz, H-6), 6.94 (1H, dd, *J* = 7.5, 1.1 Hz, H-5), 4.95 (1H, d, *J* = 7.9 Hz, H-1'), 3.92 (1H, dd, *J* = 12.0, 2.0 Hz, H-6'a), 3.76 (1H, dd, *J* = 12.0, 5.0 Hz, H-6b'), 3.62 (1H, dd, *J* = 9.2, 7.9 Hz, H-2'), 3.48 (1H, m, H-3'), 3.46 (1H, m, H-4'), 3.44 (1H, m, H-5').

^{13}C NMR (125 MHz, MeOH-d_4): δ 160.0 (CHO), 152.2 (C-4), 136.5 (C-7a), 123.4 (C-6), 115.8 (C-2), 114.6 (C-3), 112.4 (C-3a), 108.3 (C-5), 108.2 (C-7), 104.0 (C-1'), 78.2 (C-5'), 78.0 (C-3'), 75.2 (C-2'), 71.1 (C-4'), 62.3 (C-6'). ^{13}C NMR data were obtained from HMBC and HSQC spectra.

Structure elucidation

Purified compound was investigated by LC/MS and LC/MS/MS using orbitrap analyzer. Molecular peak obtained in positive ion mode provided molecular mass *m/z* 339.11655 and molecular formula $C_{15}H_{19}O_7N_2$ (mass error -2.7 ppm from theoretical mass). This $[M+H]^+$ was accompanied with *m/z* 177.06468 for which $C_9H_9ON_2$ was calculated. The mass and formula difference indicates that a hexose presence in the unknown compound. CID spectra on fixed *m/z* 177 precursor provide intense peak at *m/z* 149.07035 with calculated formula $C_8H_9ON_2$ indicating carbon monoxide loss presumably from a formyl group. Additional three less intense fragments at 159.05508, 132.04389 and 122.05972 indicates loss of water from *m/z* 177, ammonia and hydrogen cyanide from *m/z* 149. The proposed structure for unknown should contain hexose, formyl group and possess indol skeleton.

^{1}H NMR, ^{1}H-^{1}H COSY, HSQC and HMBC spectra were used for structure elucidation of 4OGlcI3F. The ^{1}H NMR spectrum, measured in MeOH-d_4 showed signals of an ABX spin

system (δ 7.09, 7.05, 6.95) and a singlet at δ 7.76 assignable to H-2, which suggested a C-3-substituted indolic compound with an additional substitution in the six-membered ring.

HMBC correlations of H-2, H-5 (δ 6.95) and H-7 (δ 7.09) with the angular C-3a (δ 112.4), H-2 and H-5 with the low-field angular C-7a (δ 136.5), and mutual HMBC correlation between H-7/C-5 (δ 108.3) and H-5/C-7 (δ 108.2) confirmed the indolic structure of the aglycon. An HMBC correlation of H-6 (δ 7.05) with the carbon atom at δ 152.2 assigned this quaternary carbon atom to position 4 and the low-field chemical shift indicated substitution by an oxygen functionality. Signals of a hexose (δ_H 4.95, 3.92, 3.76, 3.62, 3.48, 3.46, 3.44; δ_C 104.0, 78.2, 78.0, 75.2, 71.1, 62.3) which is ß-configured at the anomeric centre (J = 7.9 Hz of the doublet of H-1' at δ 4.95) were readily identified. An HMBC cross signal of H-1' with C-4 located the sugar unit at this particular carbon atom. Another singlet (δ 8.28), integrating for one proton, was attributed to a substituted methine group in an electronegative environment. According to a single HMBC correlation with a quaternary carbon atom assignable to C-3 (δ 114.6), the proton at δ 8.28 must be located in the side chain in a three bond-distance to C-3.

Based on these data, the structure of isolated compound was preliminary assigned as a 4-*O*-ß-hexosyl-indole with a N,C,O-containing side chain at C-3. The exact match of the NMR and MS data of the isolated and synthetic samples finally established the structure as 4-*O*-β-D-glucosyl-1*H*-indol-3-yl formamide (4OGlcI3F).

Synthesis of 4-*O*-ß-D-glucosyl-1*H*-indol-3-yl formamide

The compound was prepared using standard synthetic procedures of a wet chemistry and details will be published elsewhere. Analytical data of prepared compound was: ^{1}H NMR (500 MHz, d_4-MeOH): δ = 3.46 (m, 3H), 3.61 (m, 1H), 3.76 (dd, 1H, J = 12.0 and 4.9 Hz),

3.92 (dd, 1H, J = 12.0 and 2.1 Hz), 4.94 (d, 1H, J = 7.9 Hz), 6.94 (dd, 1H, J = 7.4 and 1.0 Hz), 7.04 (dd, 1H, J = 8.2 and 7.4 Hz), 7.08 (dd, 1H, J = 8.2 and 1.0 Hz), 7.75 (s, 1H), 8.27 (s, 1H). MS (ESI) *m/z* (%): $[M+Na]^+$ 361.10 (51), $[M+H]^+$ 339.12 (23), $[M+H\text{-}Glc]^+$ 177.07 (100).

Bednarek P, Pislewska-Bednarek M, Ver Loren van Themaat E, Maddula RK, Svatos A, Schulze-Lefert P (2011) Conservation and clade-specific diversification of pathogen-inducible tryptophan and indole glucosinolate metabolism in Arabidopsis thaliana relatives. New Phytol **192:** 713-726

Stein M, Dittgen J, Sanchez-Rodriguez C, Hou BH, Molina A, Schulze-Lefert P, Lipka V, Somerville S (2006) Arabidopsis PEN3/PDR8, an ATP binding cassette transporter, contributes to nonhost resistance to inappropriate pathogens that enter by direct penetration. Plant Cell **18:** 731-746

Supplemental Table S1. Segregation of the *eds* phenotype in F_2 progeny of the enhancer line 157 crossed with *pen2-1* in Ler background.

Cross	No. of *eds* plants	No. of WT plants	χ^2 (1:3)	P value
line 157 × Ler *pen2-1*	26	88	0.2924	0.5887

F_2 plants were tested for the *eds* phenotype as described in Figure 1a.
Segregation data were evaluated with the χ^2 test by using a 1:3 segregation of the *eds* phenotype as null hypothesis.

Supplemental Figure legends

Supplemental Figure S1. *pen3-5* and *pen3-4* plants support a similar level of *B. graminis* secondary hypha formation.

A, The genomic region around the *PEN3* locus (AT1G59870). The positions of DNA markers for the low-resolution mapping and the numbers of recombination for plants showing the mutant phenotype are shown (upper part). The exon-intron structure (gray boxes and black lines represent protein-coding and non-coding regions, respectively) of *PEN3* and the position of the mutation site are shown (lower part).

B, Incidence of *B. graminis* microcolonies (≥ 2 branched hyphae) of fungal germlings with a haustorium on *pen3-4*, *pen3-5* leaves, and F_1 hybrids at 2 dpi. Error bars denote standard deviations based on microscopic evaluation of at least 600 single plant-fungus interaction sites collected from four *pen3-4* and *pen3-5* plants and 20 F_1 hybrid plants.

C, *B. graminis* entry rates of germinated conidiospores on leaves of wild type, *pen3-5* and the transgenic PN:PEN3-GFP complementation lines at 2 dpi. Error bars denote standard deviations based on at least 600 fungus-plant interaction sites microscopically inspected on leaves collected from four plants. Asterisks indicate statistically significant differences between WT and mutants (**P<0.01, Student's *t* test).

D, *E. pisi* entry rates of germinated conidiospores on leaves of wild type, *pen3-5* and the transgenic PN:PEN3-GFP complementation lines at 7 dpi. Error bars denote standard deviations based on at least 600 fungus-plant interaction sites microscopically inspected on leaves collected from four plants. Asterisks indicate statistically significant differences between WT and mutants (**P<0.01, Student's *t* test).

Supplemental Figure S2. Hydrogen peroxide levels in *pen3* plants upon *G. orontii* inoculation.

Hydrogen peroxide levels in leaves of non-inoculated (white bars) and *G. orontii* inoculated plants at 3 dpi (grey bars) and 4 dpi (black bars) are indicated for each plant genotype. Error bars denote standard deviations from six plants. Asterisks indicate statistically significant differences between WT and mutants (*$p<0.05$ and ** $p<0.01$, Student's *t* test).

Supplemental Figure S3. Flg22-induced callose deposition in *pen3* mutants.

The micrographs show extracellular callose deposition in cotyledons of each indicated genotype at 24 h after flg22 treatment. Representative examples of 40 to 60 cotyledons from three independent experiments per genotype are presented. Bar = 100 μm.

Supplemental Figure S4. *pen3-5* plants are super-susceptible to the necrotrophic pathogen *Plectosphaerella cucumerina.*

A, Disease rating (DR) of the indicated genotypes inoculated with the necrotrophic fungus *P. cucumerina* strain BMM at 8 dpi. DR varies between 0 (no symptoms) and 5 (dead plant). The *cyp79b279b3* and *irx1-6* mutants (in Col-0 background), that are hypersusceptible and resistant to *P. cucumerina*, respectively, were included for comparison. Error bars denote standard deviations from three technical replicates. Asterisks indicate statistically significant differences between WT and mutants (*$p<0.05$, One-way ANOVA and Bonferroni's test).

B, qRT-PCR quantification of fungal DNA (*Pcβ-tubulin*) at 5 dpi on leaves of the indicated genotypes. Values are represented as the average of the n-fold fungal DNA

levels, relative to that on wild-type plants. Asterisks indicate statistically significant differences between WT and mutants (*P<0.05, One-way ANOVA and Bonferroni's test).

Supplemental Figure S5. NMR spectra of 4-*O*-β-D-glucosyl-1*H*-indol-3-yl formamide.

A, ^{1}H NMR spectra (500 MHz, MeOH-d_4). Isolated sample (red); synthetic sample (blue).

B, HSQC spectra (^{1}H: 500 MHz, ^{13}C: 125 MHz, MeOH-d_4). Isolated sample (left panel); synthetic sample (right panel).

C, HMBC partial spectra (^{1}H: 500 MHz, ^{13}C: 125 MHz, MeOH-d_4). Isolated sample (left panel); synthetic sample (right panel).

Supplemental Figure S6. SA hyperaccumulation in *pen3* plants is independent of PEN2 function.

A, Sporulating *G. orontii* mycelium (8 dpi) is macroscopically visible on leaves of WT and *pen2-1*, but not on *pen3-1* and *pen2-1 pen3-1* leaves. Note pathogen-inducible leaf chlorosis in *pen3-1* and *pen2-1 pen3-1* leaves. Bar = 1 cm.

B, Free SA levels in leaves of non-inoculated (white bars) and *G. orontii* inoculated plants (4 dpi, black bars) of the indicated genotypes. Error bars denote standard deviations from at least 8 plants. Asterisks indicate statistically significant differences between WT and mutants (** p<0.01, Student's *t* test).

C, Total SA levels in leaves of non-inoculated (white bars) and *G. orontii* inoculated plants (4 dpi, black bars) of the indicated genotypes. Error bars denote standard

deviations from at least 8 plants. Asterisks indicate statistically significant differences between WT and mutants (** p<0.01, Student's *t* test).

Supplemental Figure S7. PDR9 transporter is dispensable for pre-invasive defense to non-adapted powdery mildews.

A, *E. pisi* entry rates of germinated conidiospores on WT, *pdr9-2*, *pis1-1* and *pdr9-2 pen3-4* leaves at 7 dpi. Error bars denote standard deviations based on at least 600 fungus-plant interaction sites from four plants. Asterisks indicate statistically significant differences between WT and mutants (**P<0.01, Student's *t* test).

B, *B. graminis* entry rates of germinated conidiospores on WT, *pdr9-2*, *pis1-1* and *pdr9-2 pen3-4* leaves at 2 dpi. Error bars denote standard deviations based on at least 600 fungus-plant interaction sites from four plants. Asterisks indicate statistically significant differences between WT and mutants (**P<0.01, Student's *t* test).